

Supplementary Information for

Metachronal actuation of microscopic magnetic artificial cilia generates strong microfluidic pumping

Shuaizhong Zhang,^{a,b} Zhiwei Cui,^{a,b} Ye Wang,^{a,b} and Jaap M.J. den Toonder ^{*a,b}

^a Microsystems, Department of Mechanical Engineering, Eindhoven University of Technology, Eindhoven, The Netherlands. E-mail: j.m.j.d.toonder@tue.nl

^b Institute for Complex Molecular Systems (ICMS), Eindhoven University of Technology, Eindhoven, The Netherlands.

SI 1 Tuning the phase difference of the metachronal-2D motion (page S-2)

SI 2 Validation of the COMSOL simulation in Fig. 1 (page S-2)

SI 3 Magnetic field generated by the rotating magnet (page S-3)

SI 4 Bending angle of tilted conical motion (page S-3)

SI 5 Calculation of the generated volumetric flow rate and pressure drop (page S-4)

SI 6 Comparison of fluid pumping capability of our μ mac with other microfluidic pumps (page S-4)

SI 7 Local Reynolds number (page S-6)

SI 8 Supplementary movie legends (page S-7)

SI 1 Tuning the phase difference of the metachronal-2D motion

The phase difference between the beatings of adjacent μ MAC when actuated by the magnet-belt setup (Fig. 1D) can be easily tuned by changing the cilia pitch, the distance between the rod-shaped magnets, and/or the diameter of the rod-shaped magnets. Table S1 shows an example of altering the phase difference through the aforementioned means.

Table S1 Simulated results of the phase difference between adjacent cilia, by varying the cilia pitch (CP), the distance (d) between the rod-shaped magnets and the diameter of the magnets (D).

$d=0$ mm, $D=4$ mm	CP [μ m]	450	550	650
	Phase difference [$^\circ$]	20	23	28
$CP=450$ μ m, $D=4$ mm	d [mm]	0	1	2
	Phase difference [$^\circ$]	20	16	14
$d=0$ mm, $CP=450$ μ m,	D [mm]	2	4	6
	Phase difference [$^\circ$]	40	20	14

SI 2 Validation of the COMSOL simulation in Fig. 1

To validate the COMSOL simulation results in Fig. 1, we compared the experimental results of the cilia motion with the simulation results. The results are shown in Table S2. The experimental results used here are obtained from measuring the bending angle of the cilia array shown in Fig. 3A ($t = 1.2$ s). The bending angle is the angle between the cilium position shown in Fig. 3A and its upright position. A positive value indicates that the cilium position shown in Fig. 3A is to the right of its upright position, and a minus value indicates that the cilium position is to the left of its upright position. The results in Table S2 show that the experimental results agree well with simulation results during the magnetic stroke, while not for the other two strokes as expected since in reality the cilia cannot move into the substrate, like is shown in Fig. 1G.

Table S2 Comparison of experimental results and COMSOL simulation results regarding the cilia motion when the cilia are actuated by the magnet-belt

Beating cycle		Magnetic stroke					Sliding stroke			Elastic stroke	
Bending angle [$^\circ$]	Simulation results	0	20	40	60	80	99	119	140	160	-178
	Experimental results	-1	19	34	44	56	65	80	90	90	-4
Phase difference [$^\circ$]	Simulation results	20	20	20	20	19	20	21	20	18	
	Experimental results	20	15	10	12	9	15	10	0	94	

SI 3 Magnetic field generated by the rotating magnet

The magnetic field experienced by the μ MAC during one cycle when they are actuated by the rotating magnet setup (Fig. 2B) is depicted in Fig. S1. Details about the calculation of the magnetic field are available in an earlier paper.²⁵

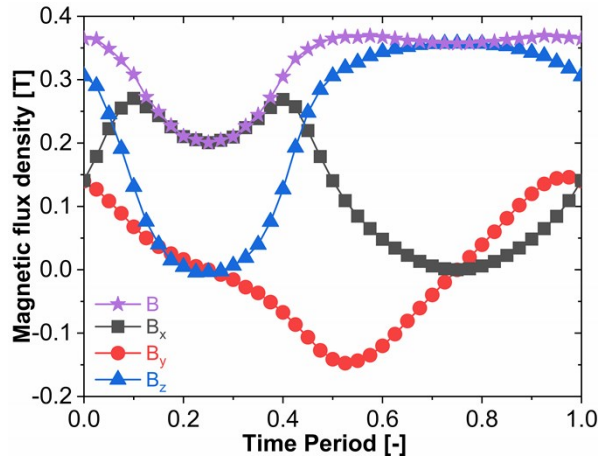


Fig. S1 Magnetic field experienced by the μ MAC during one cycle when they are actuated by the rotating magnet setup shown in Fig. 2B. Details are available in an earlier paper.²⁵

SI 4 Bending angle of tilted conical motion

The maximum bending angle ϑ of the tilted conical motion (Fig. S2) was calculated from the tips' projected displacement with the assumption that the cilia are rigid rods that only bend at the anchor points. Hence $\sin \vartheta = \text{tips' projected displacement} / \text{the length of the cilia}$.

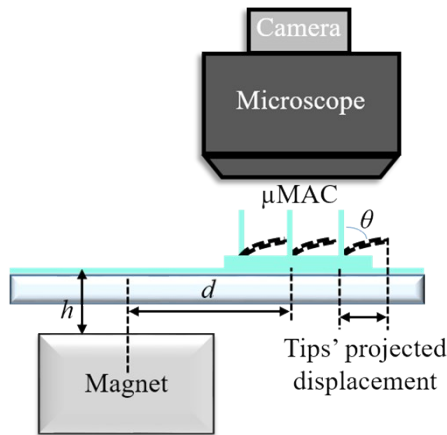


Fig. S2 Schematic of the setup for measuring the bending angle of the tilted conical motion with a CMOS camera (DFK 33UX252) mounted on a microscope (Olympus SZ61) for capturing cilia deformation. The permanent magnet is the same as the rotating magnet used in the actuation setup in Fig. 2B. The vertical distance h and horizontal distance d between the magnet and the cilia is 2 and 13 mm,

respectively. This arrangement corresponds to the situation when the magnet in Fig. 2B rotates 180°. Illustration is not to scale.

SI 5 Calculation of the generated volumetric flow rate and pressure drop

When the maximum velocity within the microfluidic channel at actuation frequency f is known, the corresponding volumetric flow rate Q_f and the pressure drop ΔP_f (which is the pressure difference between the locations right before and after the ciliated area) generated by the μ MAC can be calculated as follows:

$$\Delta P_f = \frac{\eta v_{xf}(0, 0)L\pi^3}{4w^2 \sum_{i=1,3,5,\dots}^{\infty} (-1)^{\frac{i-1}{2}} \left[1 - \frac{1}{\cosh\left(\frac{i\pi h}{2w}\right)} \right] \frac{1}{i^3}} \quad (S1)$$

$$Q_f = \frac{\Delta P_f h w^3}{12\eta L} \left[1 - \frac{192w}{\pi^5 h} \sum_{i=1,3,5,\dots}^{\infty} \frac{\tanh\left(\frac{i\pi h}{2w}\right)}{i^5} \right] \quad (S2)$$

where η is the dynamic viscosity of the liquid at room temperature (1 mPa·s for water and 1.4 Pa·s for glycerol), $v_{xf}(0, 0)$ is the measured flow speed in the geometrical center of the channel at the actuation frequency of f , w is the width of the channel, h is the height of the channel, L is the length of the channel.²⁵ In our study, $w = 5$ mm, $L = 10\pi - 4 = 31.4 - 4 = 27$ mm, $h = 660$ μ m. The calculated flow rate and pressure drop are depicted in Fig. S3 and Fig. 4B, respectively.

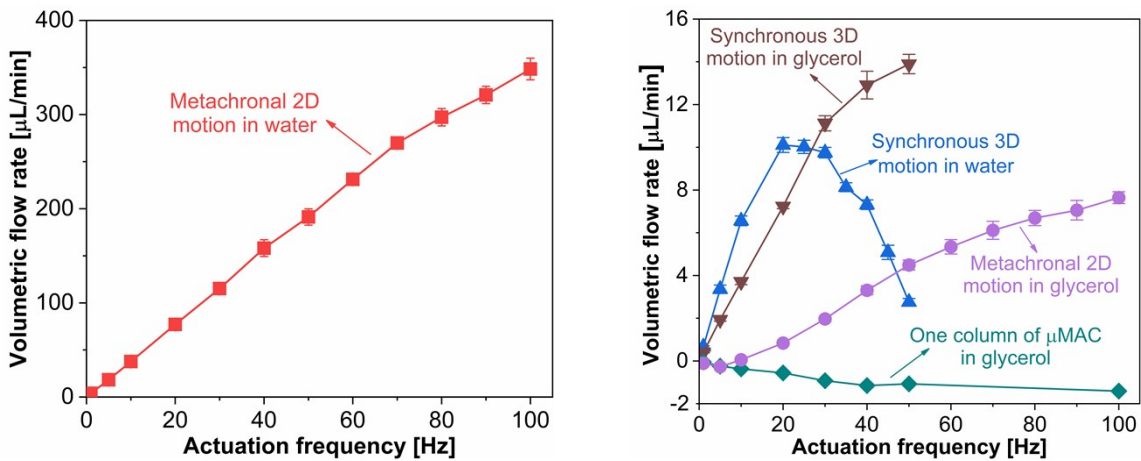


Fig. S3 Corresponding volumetric flow rate generated by the μ MAC. All error bars are standard deviations of the obtained data of at least five measurements.

SI 6 Comparison of fluid pumping capability of our μ mac with other microfluidic pumps

Our μ MAC are capable to generate a water volumetric flow rate Q_{max} of $350 \mu\text{L min}^{-1}$ when performing the metachronal motion in the circular channel with radius 5 mm, and with a rectangular cross section that is $660 \mu\text{m}$ high and 5 mm wide, at an actuation frequency of 100 Hz (see Fig. S3). Comparing the flow rate to those that have been achieved using electro-hydrodynamic and electroosmotic pumping methods (reviewed by Laser and Santiago³⁹), our cilia-based pumping is in the upper range, see Fig. S4A. However, this comparison is for widely different channel sizes, and to account for this, Laser and Santiago have defined the “self-pumping performance”, Q_{max}/S_p as a parameter that can be used to characterize and compare micropumping efficiencies; S_p is the total volume of the channel.³⁹ Our circular channel has a total volume S_p of 104 mm^3 , which gives a self-pumping performance of 3.4 min^{-1} . Fig. S4B shows that our μ MAC, actuated to perform metachronal 2D motion, is in the upper range of self-pumping performance compared with the other methods of microfluidic pumping reviewed by Laser and Santiago³⁹ while the size is one of the smallest.

Finally, a comparison between our μ MAC and previously published artificial cilia is summarized in Table S2. It can be concluded that our μ MAC outperform all reported artificial cilia in terms of generated flow speed, except for the millimeter-size pneumatic cilia.³⁴

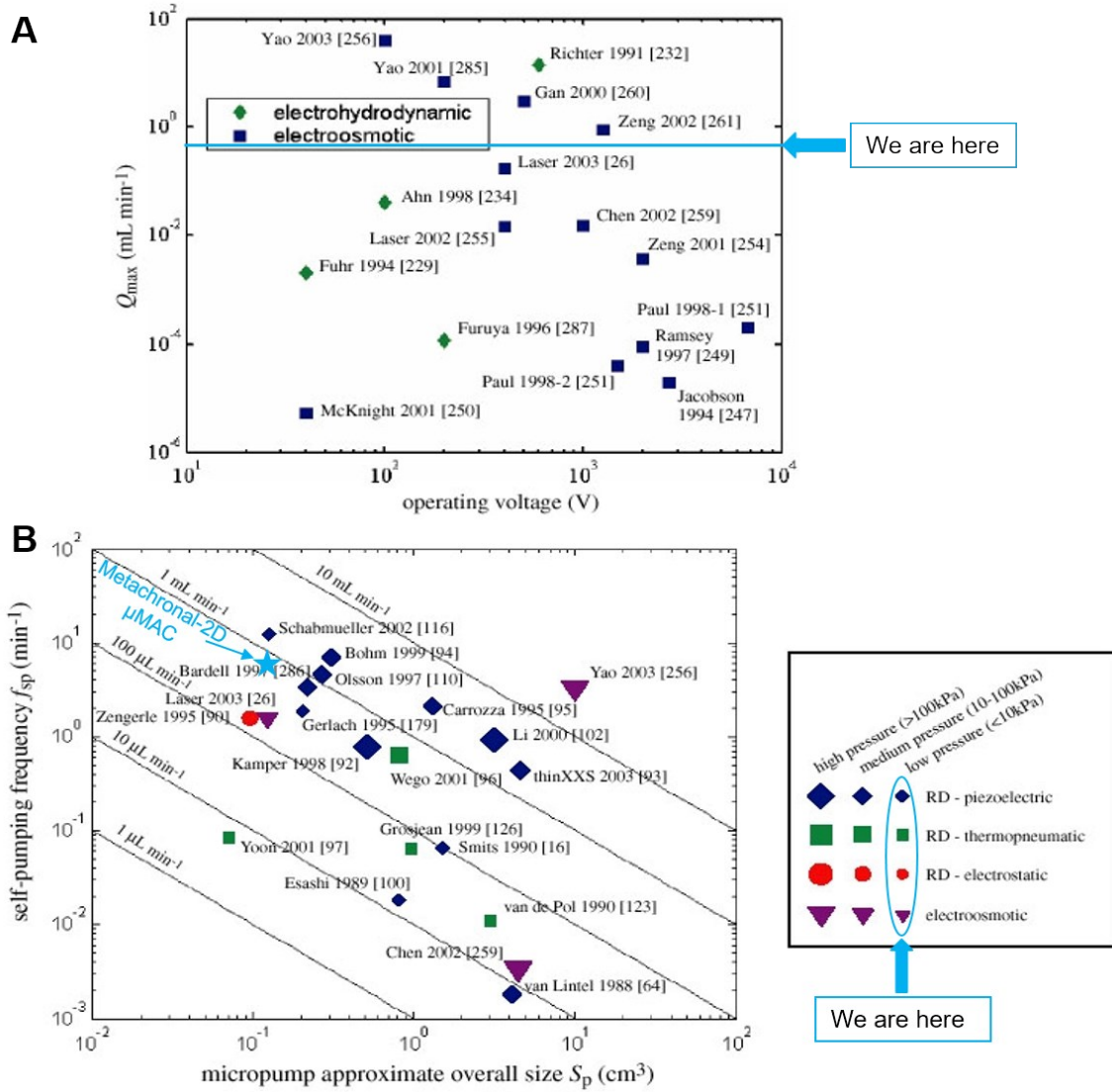


Fig. S4 Comparison of the performance of the μ MAC actuated to perform metachronal 2D motion in water with reported micropumps. (A) The volumetric flow rate compared with electro-hydrodynamic and electroosmotic pumping. (B) Comparison of the self-pumping frequency and size for a range of micropumps; the size of the data point marker indicates the associated ΔP . Reproduced from Laser and Santiago³⁹ with our data inserted.

Table S3. Comparison between our metachronal μ MAC (italic) and previously published artificial cilia in terms of fluid pumping in water unless otherwise specified, with the best one highlighted in bold font. In the table, these artificial cilia are arranged in terms of their length from low to high. ‘-’ means the data is not given.

Cilia type	Cilia length [μm]	Maximum flow speed [μm s ⁻¹]	Maximum flow rate [μL min ⁻¹]	Maximum pressure drop [Pa]
Self-assembled cilia ⁴³	20	3	-	-
<i>μMAC²⁰</i>	25	8	28	-

Self-assembled cilia ¹⁹	31	5	-	-
μ MAC ²¹	70	-	18	-
Electrostatic cilia ^{*17}	100	600	-	-
μ MAC ²⁴	200	1350	11	1
μ MAC ²³	250	120	0.7	-
μ MAC ²²	300	70	0.6	0.04
μ MAC ²⁵	350	260	40	0.65
<i>Our synchronous-3D μMAC</i>	350	90	10	0.04
<i>Our metachronal-2D μMAC</i>	350	3000	350	1.5
Metachronal MAC ^{**9}	4000	83	-	-
Pneumatic metachronal-2D cilia ³⁴	8000	19000	-	-

*working fluid: silicone oil; **working fluid: glycerol.

SI 7 Local Reynolds number

The local Reynolds number is defined by $Re = \rho v L / \eta$, in which ρ is the density of the fluid at room temperature, v is the maximal speed of the cilia tips at the actuation frequency f (see Fig. 5 A and D, and Fig. S5A), L is the characteristic length for which we take the cilia length (350 μ m in our experiments), and η is the dynamic viscosity of the fluid at room temperature (1 mPa·s for water and 1.4 Pa·s for glycerol). The calculated Re is plotted in Fig. S5B as a function of actuation frequency.

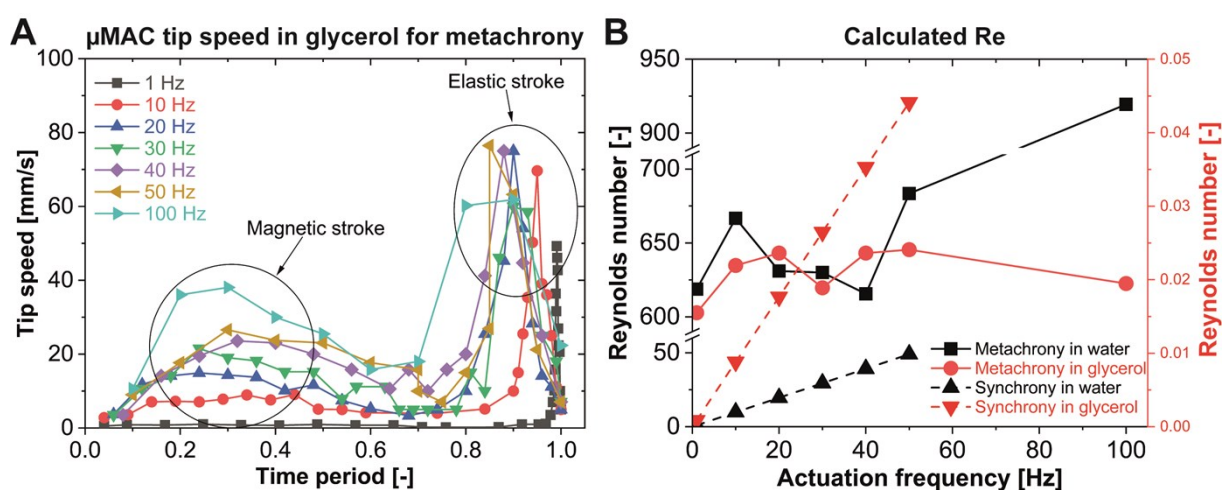


Fig. S5 Quantitative analyses of the μ MAC motion. **(A)** Tip speed in glycerol during one beating cycle when the μ MAC are actuated by the magnet-belt. **(B)** Calculated Reynolds number (Re) based on cilia tip's maximal speed. The black lines correspond to the left y-axis and the red lines correspond to the right y-axis.

SI 8 Supplementary movie legends

All experimental movies were recorded using a high-speed camera (Phantom V9) mounted on a stereo microscope (Olympus SZ61). The μ MAC in the movies have a diameter of 50 μm , a height of 350 μm and a pitch of 450 μm . The white particles are 12 μm polystyrene tracer particles (micromod Partikeltechnologie GmbH).

Movie ESI 1 A high-speed video showing the metachronal motion of one row of μ MAC in both water and glycerol from both side view and top view at 1 Hz.

Movie ESI 2 A high-speed video showing the cilium motion during the elastic stroke in both water and glycerol from side view at 1 Hz.

Movie ESI 3 A high-speed video showing the tilted conical motion of the μ MAC in both water and glycerol from top view at 50 Hz.

Movie ESI 4 A high-speed video showing the weakened metachronal motion of one row of μ MAC in glycerol from side view at 50 Hz and 100 Hz. Note that the third cilium from the left of the movie shows different behavior from the others due to some damage.

Movie ESI 5 A high-speed video showing the local water backflow near the ciliated area when the μ MAC are actuated to perform the tilted conical motion at 40 Hz in the circular chip shown in Fig. 2A. The direction of the effective stroke is upwards.

Movie ESI 6 A high-speed video showing the direction reversible water flow generated by the metachronal motion at 20 Hz.

Movie ESI 7 A high-speed video showing the oscillating water flow generated by the metachronal motion at actuation frequencies between -40 Hz and 40 Hz.

Movie ESI 8 A high-speed video showing the pulsatile water flow generated by the metachronal motion at actuation frequencies between 0 and 40 Hz.